Electronic Supplementary Material (ESI) for Journal of Materials Chemistry C.

Supporting Information

A Silanol-Functionalized Polyoxometalate with Excellent Electron Transfer Mediating Behavior to ZnO and TiO_2 Cathode Interlayers for Highly Efficient and Extremely Stable Polymer Solar Cells

Marinos Tountas,[a,b] Yasemin Topal,[c] Apostolis Verykios,[a,d] Anastasia Soultati,[a] Andreas Kaltzoglou,[a] Theodoros A. Papadopoulos,[e] Florian Auras,[f] Kostas Seintis,[d] Mihalis Fakis,[d] Leonidas C. Palilis,[d] Dimitris Tsikritzis,[g] Stella Kennou,[g] Azhar Fakharuddin,[h] Lukas Schmidt-Mende,[h] Spyros Gardelis,[i] Mahmut Kus,[j] Polycarpos Falaras,[a] Dimitris Davazoglou,[a] Panagiotis Argitis,[a] Maria Vasilopoulou[a,]*

[a]*Institute of Nanoscience and Nanotechnology, National Centre for Scientific Research "Demokritos", 15310, Agia Paraskevi, Attiki, Greece*

[b]*School of Applied Mathematical and Physical Sciences, National Technical University of Athens, Zografou Campus, 15780 Athens, Greece*

[c]*Pamukkale University Cal Vocational High School,20700, Cal/Denizli, Turkey.*

[d]*Department of Physics, University of Patras, 26504 Patras, Greece*

[e]*Department of Natural Sciences, University of Chester, Thornton Science Park, CH2 4NU, Chester, U. K.*

[f]*Cavendish Laboratory, University of Cambridge, Cambridge CB3 0HE, United Kingdom*

[g]*Department of Chemical Engineering, University of Patras, 26504 Patras, Greece*

[h]*Department of Physics, University of Konstanz, 78457 Konstanz, Germany.*

[i]*Solid State Physics Section, Physics Department, National and Kapodistrian University of Athens, Panepistimioupolis, 15784 Zografos, Athens, Greece*

[j]*Chemical Engineering Department, Selcuk University, 42075 Konya, Turkey*

**email: m.vasilopoulou@inn.demokritos.gr*

Additional Figures

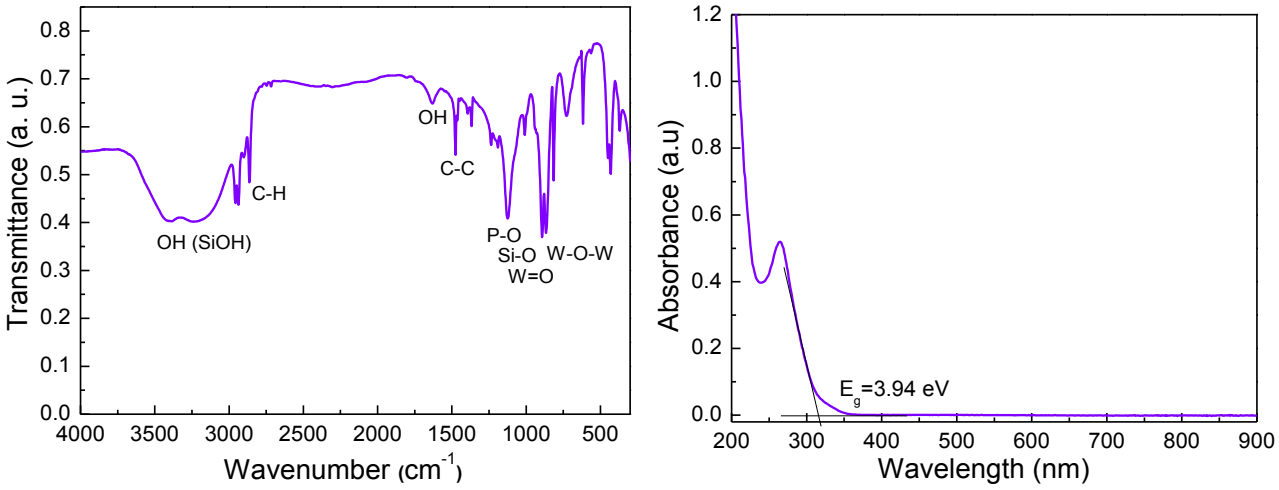

(a) **(b)**

Figure S1 (a) FTIR spectrum of tBuSiOH-POM. For the POM part, the bands at 1100 cm^{-1} and 1034 cm^{-1} are assigned to the P-O stretching modes of the central PO_4 tetrahedron.[1] At 1003 cm^{-1}, 969 cm^{-1}, 940 cm^{-1} appear bands corresponding to W=O modes and at 864 cm^{-1}, 835 cm^{-1}, 727 cm^{-1} corresponding to W-O-W stretching modes, while the bands at 389 cm^{-1} and 345 cm^{-1} are considered as the α isomer signature.[2] The bands at 810 cm^{-1} and 1080 cm^{-1} are assigned to Si-O bending and stretching modes while the band at 1487 cm^{-1} is assigned to C-C stretching mode.[3] In the high-frequency part, the typical broad-band pattern at 3400 cm^{-1} is characteristic of the –OH stretching of Si-OH or adsorbed water molecules.[4] (b) Absorption spectrum of tBuSiOH-POM in an acetonitrile solution.

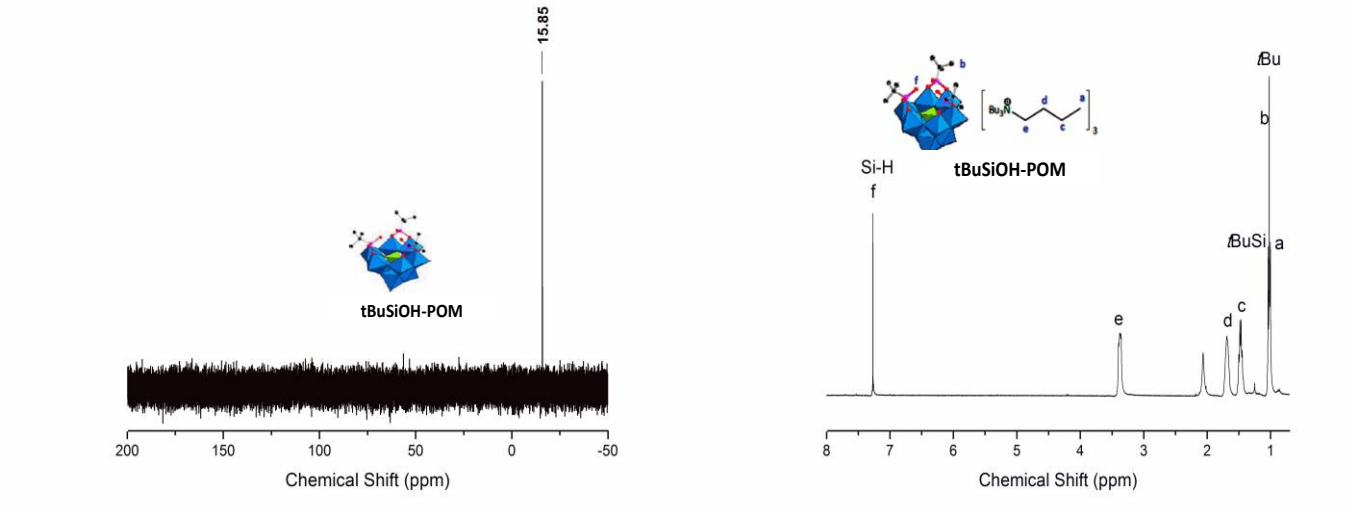

(a) **(b)**

Figure S2 (a) ^{31}P NMR and (b) ^{1}H NMR spectra of tBuSiOH-POM: The ^{31}P NMR spectrum depends on the saturation state of the polyoxometalate.[5] In the case of tBuSiOH-POM, the signal for the phosphorus atoms is found at δ =-15.85 ppm. For a complete structural analysis in solution of tBuSiOH-POM, ^{1}H NMR spectroscopy has been performed in CD_3CN. In addition to the $[nBu_4N]^+$ resonances, the ^{1}H NMR spectrum of tBuSiOH-POM displays assigned to the Si-OH and tBuSi moieties respectively. The relative integration of these signals compatible with the formula, that are three tBuSiOH groups grafted on a $[PW_9O_{34}]^{9-}$ anion and there are $[nBu_4N]^+$ cations.[6,7.]

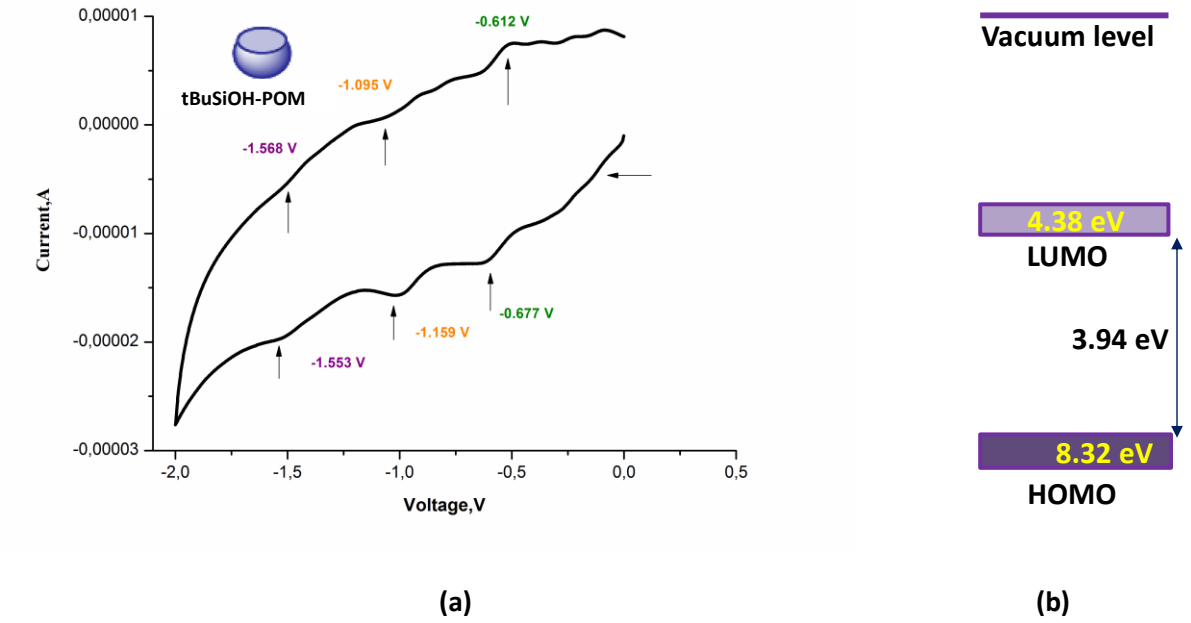

(a) **(b)**

Figure S3 (a) Cyclic voltammogram of tBuSiOH-POM at glassy carbon electrode. The concentration of tBuSiOH-POM was 10^{-3} mol L^{-1} in a acetonitrile solution with 10^{-1} mol L^{-1} Bu_4NBF_4 as supporting electrolyte. Scanning rate: 100 mV/s. The cyclic voltammetry data of the tBuSiOH-POM compound were collected with respect to Ag/Ag^+ and the calculated LUMO energy level was -4.384 eV. Notably, each of the three polyoxotungstate hybrids $[PW_9O_{34}(tBuSiOH)_3]^{3-}$ displays three reversible waves. They correspond to one-electron redox processes as it is known to be the case for Keggin-type POMs in non-aqueous solvents when no protonation accompanies reduction.[8,9] The reduction waves of tBuSiOH-POM are only slightly shifted to more negative potentials with respect to $[PW_9O_{34}(tBuSiOH)_3]^{3-}$. (b) Energy levels of POM as estimated from cyclic voltammetry and absorption measurements.

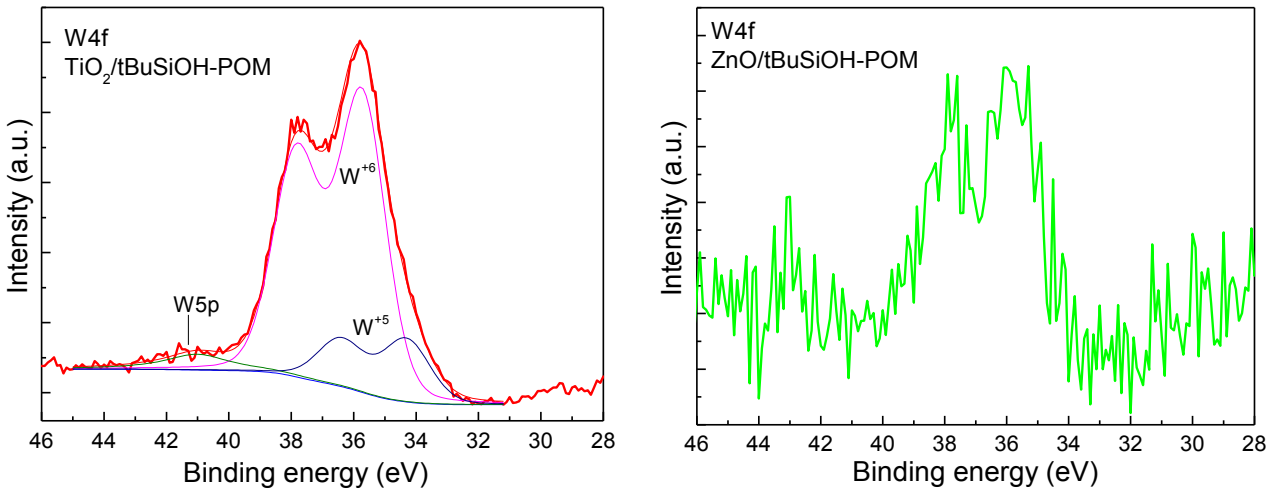

(a) **(b)**

Figure S4 XPS W4f peaks of a tBuSiOH-POM thin film deposited on (a) TiO_2 and (b) ZnO substrates. The deconvolution of the W 4f photoemission peaks of tBuSiOH-POM on TiO_2 was performed using two distinct doublets with the major contribution coming from the doublet with peaks of nearly equal width with the binding energy (BE) of W $4f_{7/2}$ centered at 35.8 ± 0.1 eV and that of W $4f_{5/2}$ at a BE of 37.8 ± 0.1 eV (with a peak ratio of 4:3). The position and the shape of these peaks are representative of W atoms with an oxidation state +6.[10] In addition, a second doublet at lower BEs (BE of W $4f_{7/2}$ = 34.5 eV, and of W $4f_{5/2}$ = 36.2 eV with a peak ratio 4:3) is also evident, which was attributed to the presence of W^{5+} ions, indicating that these films are reduced (exhibiting tungsten atoms with a valence of +5). The signal of tBuSiOH-POM on ZnO was very weak probably due to the nanoparticle-like surface morphology and the increased surface roughness of ZnO as compared to TiO_2.

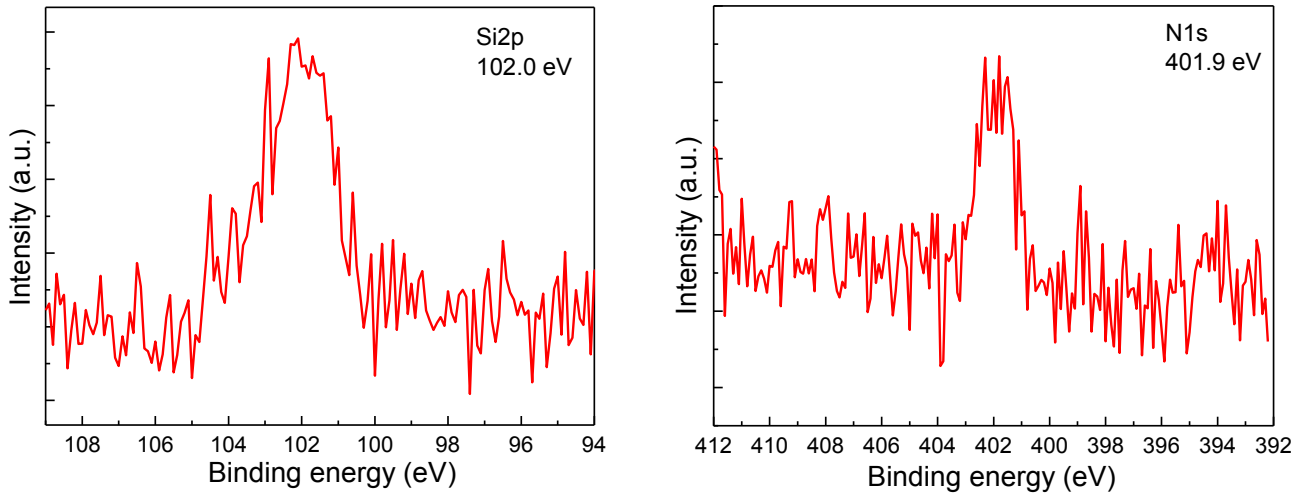

(a) **(b)**

Figure S5 XPS spectra acquired from TiO_2/tBuSiOH-POM interface of (a) Si2p and (b) N1s located at 102.0 eV and 401.9 eV BEs respectively. The signal of the corresponding XPS peaks of ZnO/tBuSiOH-POM interface was very weak and, therefore, they are not presented.

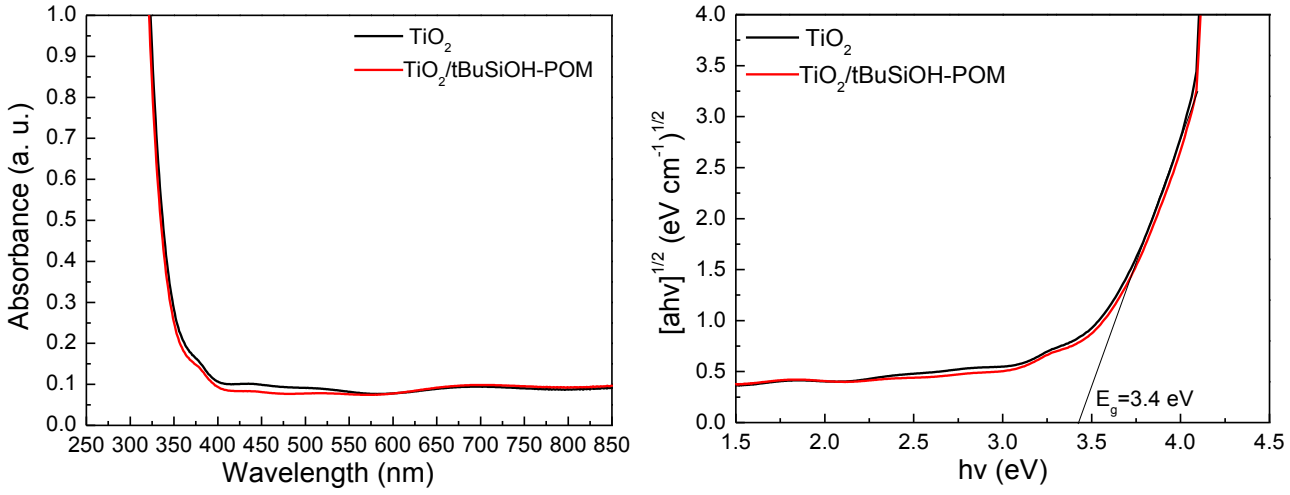

Figure S6 (a) Absorption spectra and (b) Tauc plots as derived from absorption measurements for TiO_2 (indirect gap) with and without the tBuSiOH-POM.

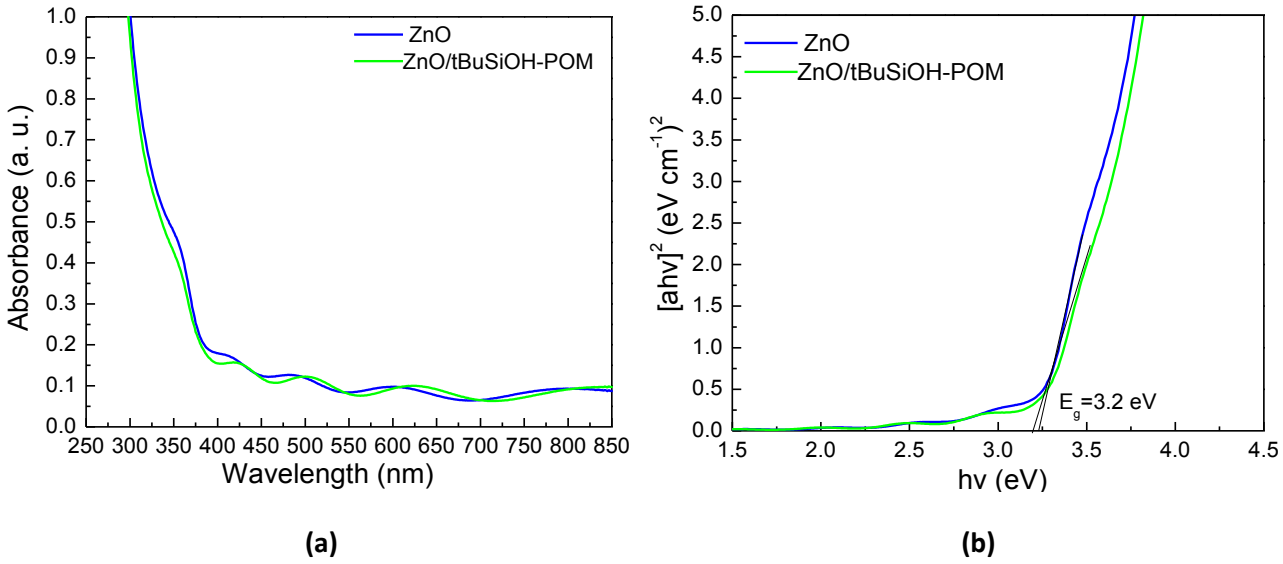

Figure S7 (a) Absorption spectra and (b) Tauc plots as derived from absorption measurements for ZnO (direct gap) with and without the tBuSiOH-POM.

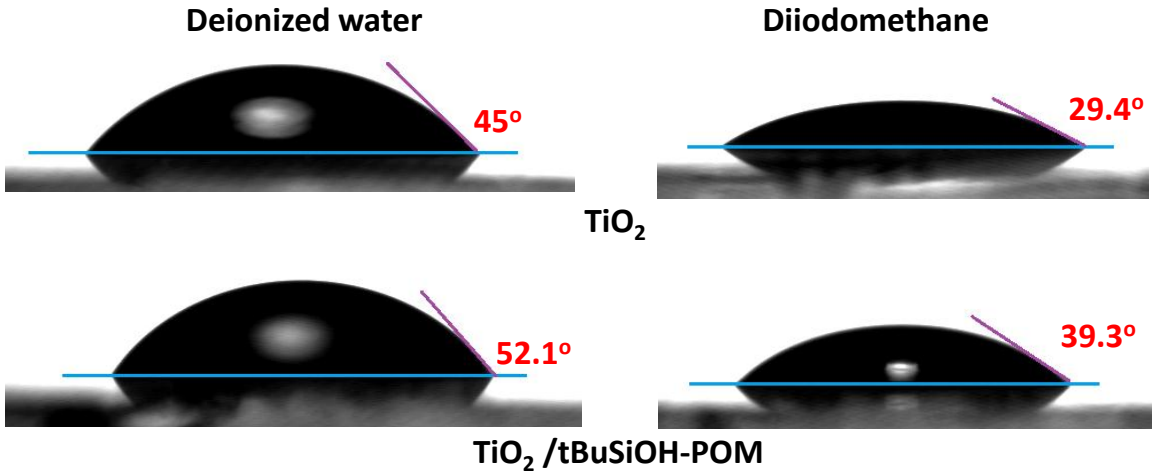

Figure S8 Contact angle measurements of deionized water and diiodomethane drops on TiO_2 with and without tBuSiOH-POM.

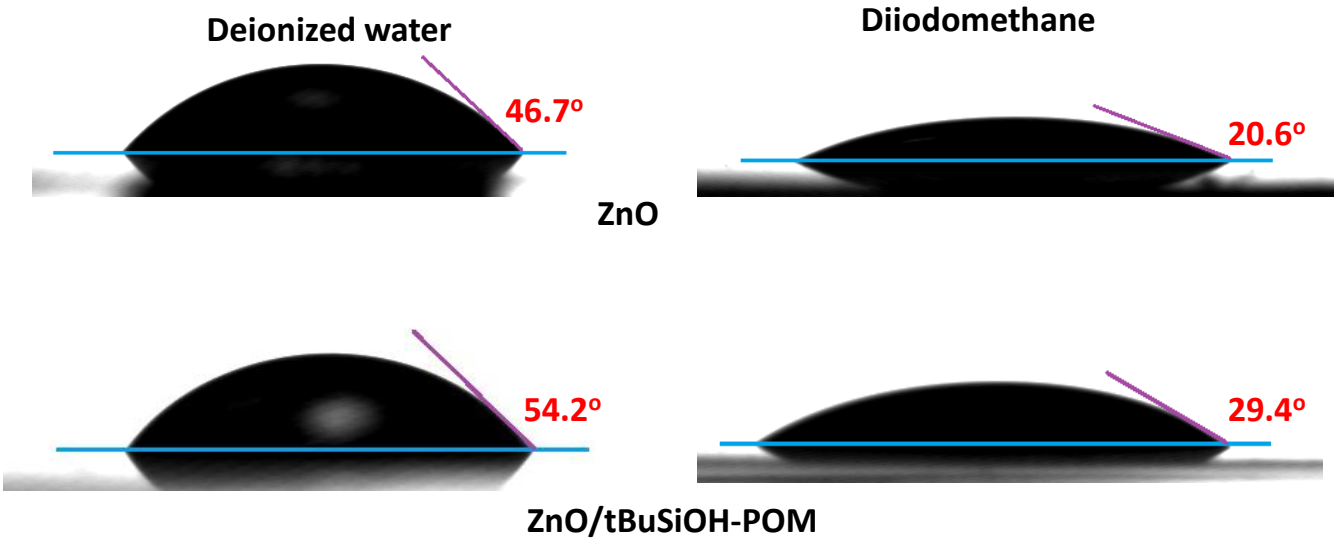

Figure S9 Contact angle measurements of deionized water and diiodomethane drops on ZnO with and without tBuSiOH-POM.

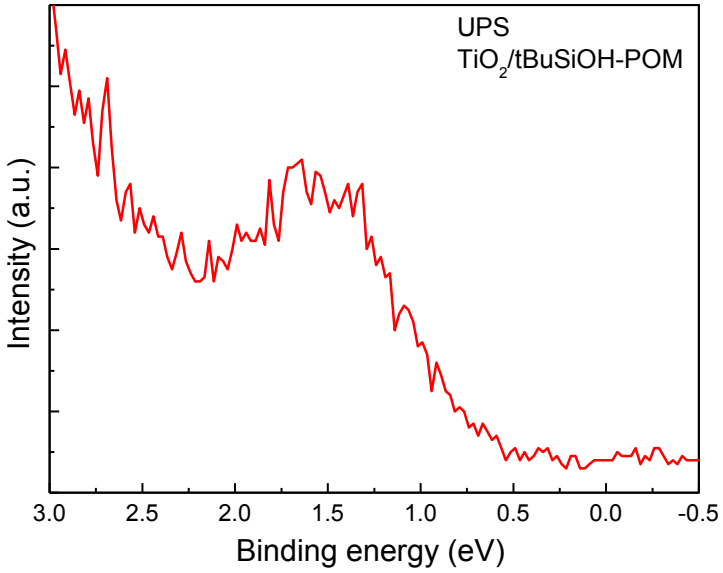

Figure S10 The near Fermi level region of the UPS spectrum of TiO_2/tBuSiOH-POM interface.

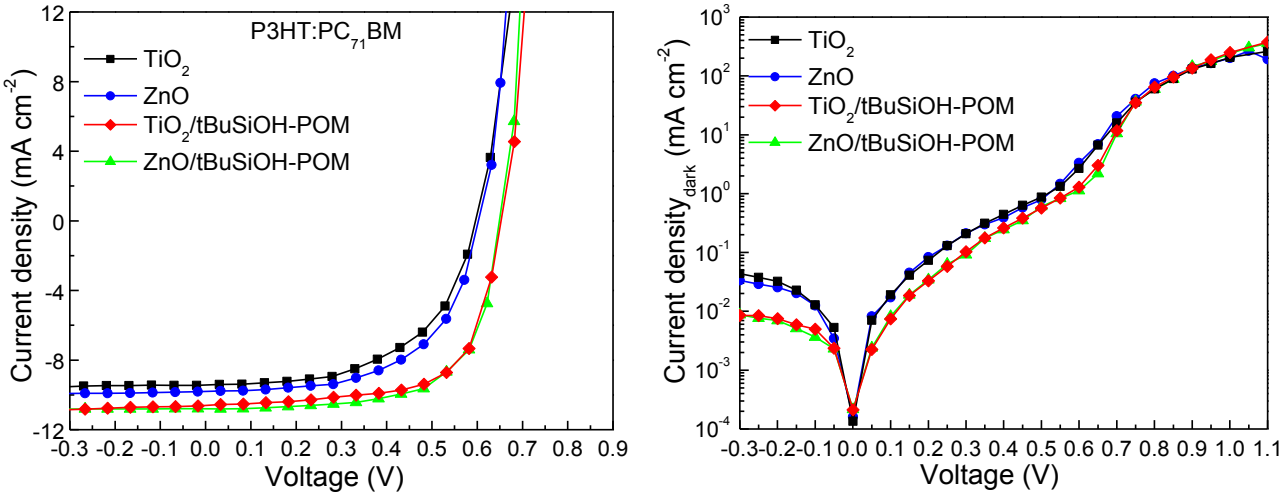

(a) **(b)**

Figure S11 (a) J-V characteristics under 1.5 AM illumination of P3HT:PC_{71}BM-based devices fabricated on FTO/TiO_2 or FTO/ZnO substrates without and with tBuSiOH-POM (see also Table S2). For the device fabrication P3HT:PC_{71}BM blends (10 mg mL^{-1} for P3HT, 8 mg mL^{-1} for PC_{71}BM in 1,2-dichlorobenzene) were spin coated at 600 rpm for 40 sec and annealed at 135 ^{o}C for 15 sec. (b) Dark J-V characteristics of the PSC devices without and with tBuSiOH-POM.

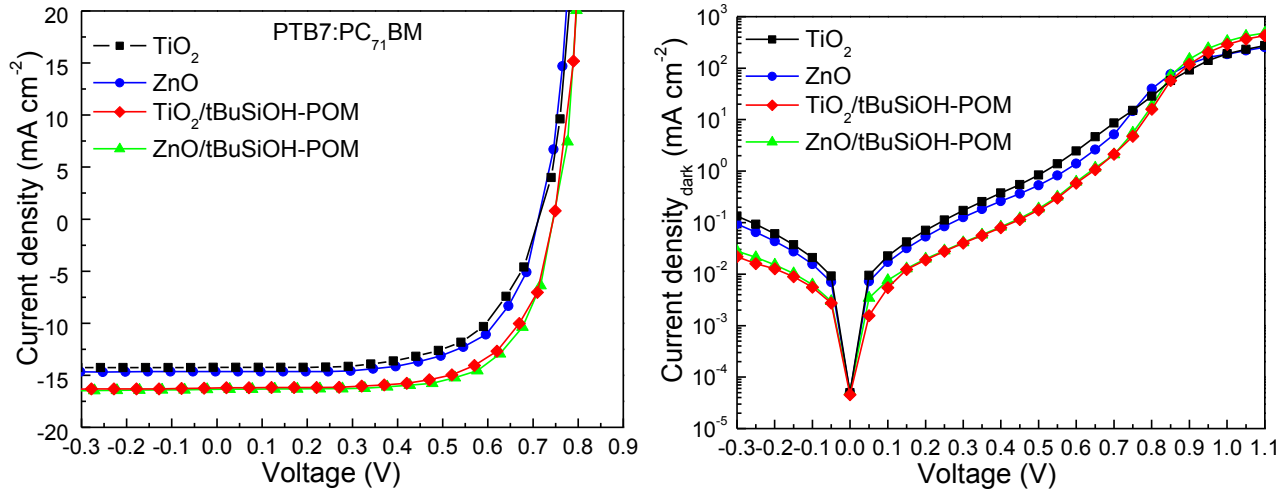

Figure S12 J-V characteristics under 1.5 AM illumination of PTB7:$PC_{71}BM$-based devices fabricated on FTO/TiO_2 or FTO/ZnO substrates without and with tBuSiOH-POM (see also Table S3). For the device fabrication PTB7:$PC_{71}BM$ blends were deposited inside an argon filled glove-box via spin coating at 1000 rpm for 90 sec from solutions with concentrations of 10 mg mL^{-1} for PTB7 and 15 mg mL^{-1} for $PC_{71}BM$ in 1,2-dichlorobenzene where 3% per volume of 1,8-diiodoctane (DIO) was added and was then left to dry for 30 min inside the glove box, without any post-deposition annealing. (b) Dark J-V characteristics of the PSC devices without and with tBuSiOH-POM.

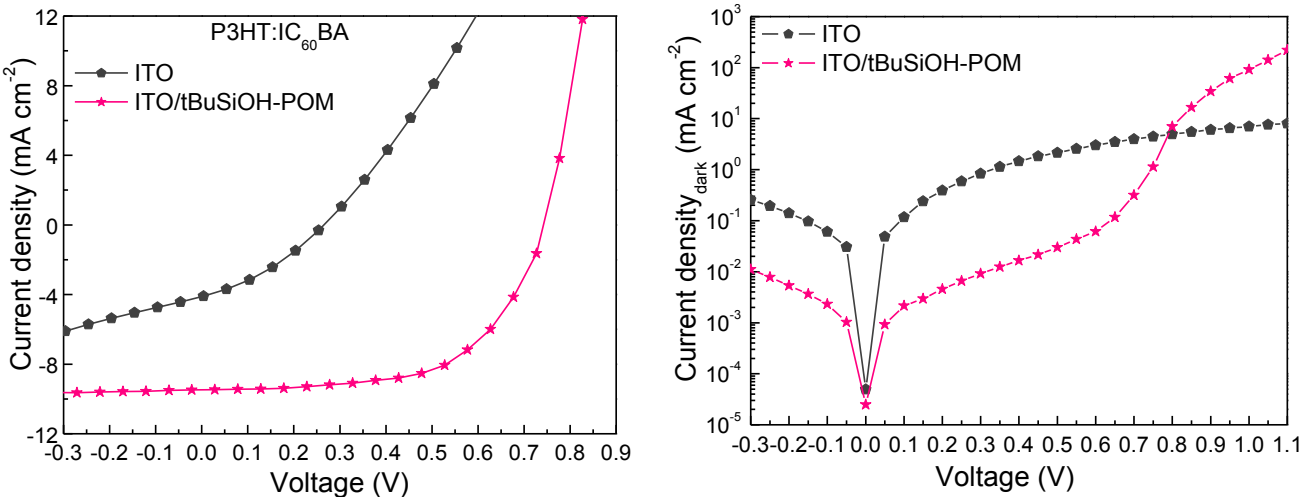

Figure S13 (a) J-V characteristics under 1.5 AM illumination of P3HT:$IC_{60}BA$-based devices fabricated on ITO and ITO/tBuSiOH-POM substrates (see also Table S4). (b) Dark J-V characteristics of the PSC devices without and with tBuSiOH-POM.

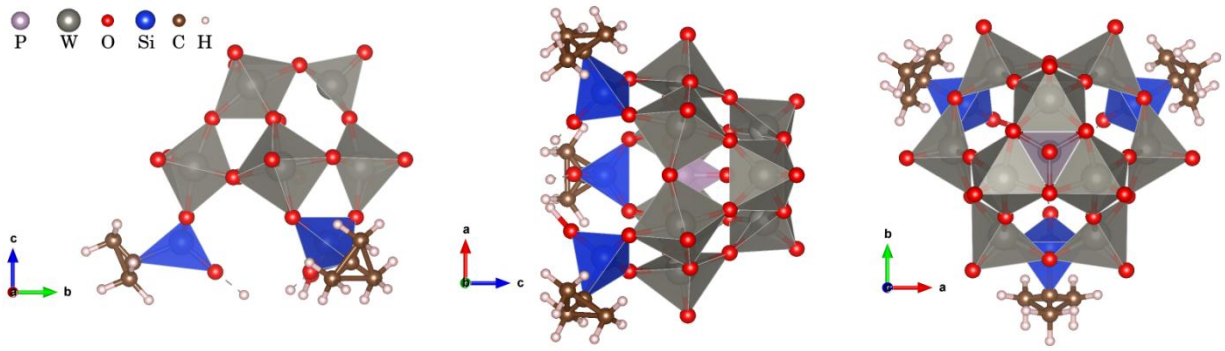

Figure S14 Polyhedral molecular structure of the tBuSiOH-POM in gas phase, obtained via geometry optimization at the DFT-PBE level of theory.

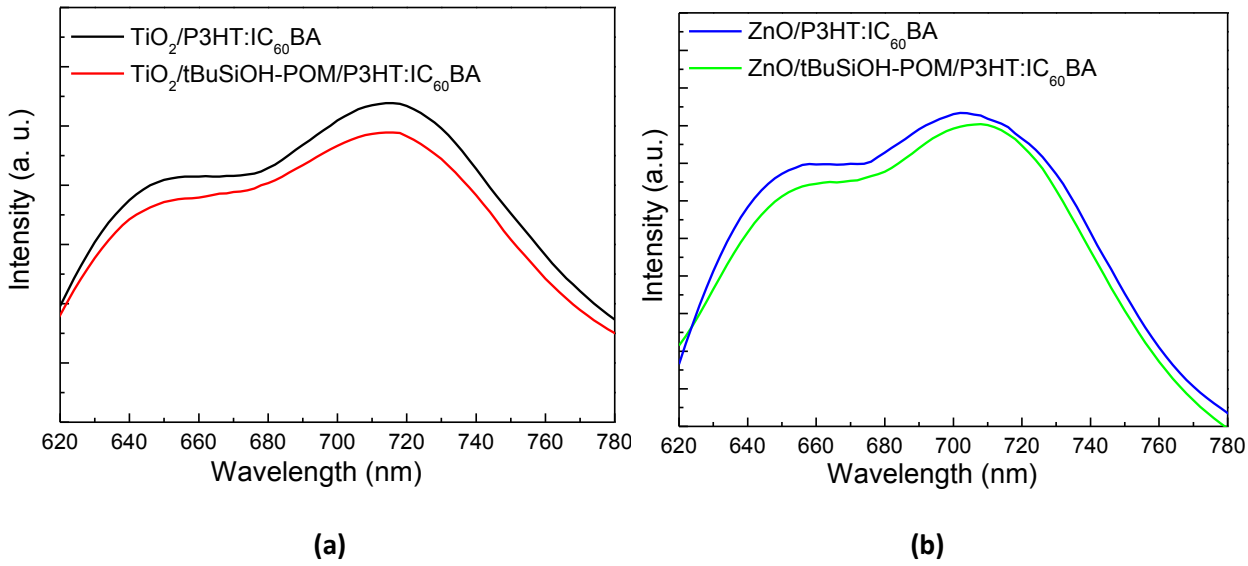

Figure S15 Steady-state PL spectra of P3HT:IC_{60}BA blends on as-deposited and tBuSiOH-POM-covered (a) TiO_2 and (b) ZnO films.

Additional tables

Table S1 Surface energy as derived from contact angle measurements of TiO_2 and ZnO substrates without and with tBuSiOH-POM spin coated from a solution with concentration of 5 mg ml^{-1}.

Substrate	θ_w (^{o})	θ_i (^{o})	γ_{sp} (mJ m^{-2})	γ_{sd} (mJ m^{-2})	γ(mJ m^{-2})
TiO_2	45.0 (±2.0)	29.4 (±1.0)	22.93 (±0.53)	35.81 (±0.07)	58.74 (±0.40)
TiO_2/tBuSiOH-POM	52.1 (±1.8)	39.3 (±1.2)	20.40 (±0.75)	32.22 (±0.40)	52.62 (±0.45)
ZnO	46.7 (±2.1)	20.6 (±0.9)	20.21 (±0.71)	39.26 (±0.27)	59.47 (±0.43)
ZnO/tBuSiOH-POM	54.2 (±1.8)	29.4 (±1.0)	16.75 (±0.50)	37.18 (±0.30)	53.93 (±0.20)

TableS2. Device characteristics of polymer solar cells having the device configuration FTO/TiO_2 or ZnO without and with tBuSiOH-POM/P3HT:$PC_{71}BM$/MoO_x/Al (mean values and standard deviations were extracted from a batch of 8 independent devices).

ETL	J_{sc} (mA cm^{-2})	V_{oc} (V)	FF	PCE (%)	R_s (Ω cm^2)	R_{sh} (Ω cm^2)
TiO_2	9.43 (±0.11)	0.60 (±0.01)	0.56 (±0.01)	3.17 (±0.12)	3.9	1807
ZnO	9.80 (±0.10)	0.60 (±0.01)	0.58 (±0.01)	3.41 (±0.10)	2.8	1763
TiO_2/tBuSiOH-POM	10.60 (±0.15)	0.64 (±0.01)	0.65 (±0.01)	4.41 (±0.14)	2.1	2667
ZnO/ tBuSiOH-POM	10.80 (±0.12)	0.64 (±0.01)	0.64 (±0.01)	4.42 (±0.13)	1.9	2376

TableS3. Device characteristics of polymer solar cells having the device configuration FTO/TiO_2 or ZnO without and with tBuSiOH-POM/PTB7:$PC_{71}BM$/MoO_x/Al (mean values and standard deviations were extracted from a batch of 8 independent devices).

ETL	J_{sc} (mA cm^{-2})	V_{oc} (V)	FF	PCE (%)	R_s (Ω cm^2)	R_{sh} (Ω cm^2)
TiO_2	14.24 (±0.17)	0.71 (±0.01)	0.63 (±0.01)	6.37 (±0.15)	2.4	2677
ZnO	14.64 (±0.14)	0.71 (±0.01)	0.64 (±0.01)	6.65 (±0.16)	2.0	3674
TiO_2/tBuSiOH-POM	16.20 (±0.16)	0.74 (±0.01)	0.67 (±0.01)	8.03 (±0.17)	1.8	3921
ZnO/ tBuSiOH-POM	16.35 (±0.13)	0.74 (±0.01)	0.68 (±0.01)	8.23 (±0.14)	1.5	4361

TableS4. Device characteristics of polymer solar cells having the device configuration ITO without and with tBuSiOH-POM/P3HT:$IC_{60}BA$/MoO_x/Al (mean values and standard deviations were extracted from a batch of 4 independent devices).

ETL	J_{sc} (mA cm^{-2})	V_{oc} (V)	FF	PCE (%)	R_s (Ω cm^2)	R_{sh} (Ω cm^2)
ITO	3.69 (±0.18)	0.25 (±0.01)	0.31 (±0.01)	0.29 (±0.20)	21.2	123
ITO/tBuSiOH-POM	9.51 (±0.14)	0.74 (±0.01)	0.60 (±0.01)	4.22 (±0.17)	3.7	1620

Table S5 Fitting parameters, obtained for P3HT 20 nm thick films (excitation wavelength: 410 nm. Detection wavelength: 700 nm) deposited on TiO_2 or ZnO substrates without and with tBuSiOH-POM.

Substrate	A_1	τ_1 (ps)	A_2	τ_2 (ps)	A_3	τ_3 (ps)	<τ> (ps)
TiO_2	-	-	0.63	2.2	0.37	16	7.4
TiO_2/tBuSiOH-POM	0.47	0.32	0.53	1.91	-	-	1.2
ZnO	-	-	0.61	2.9	0.39	22	10.3
ZnO/ tBuSiOH-POM	0.31	1.5	0.37	3.2	0.32	23	9.0

Additional references

1. U. Lavrencic-Stangar, N. Groselj, B. Orel, P. Colomban, *Chem. Mater.*, 2000, **12**, 3745-3753.
2. A. Jalil, M. Al-Daous, A. Al-Arfaj, A. Al-Amer, J. Beltramini, S. Barri, *Appl. Catal.* A, 2001, **207**, 159-171.
3. A. Mazeaud, N. Ammari, F. Robert, R. Thouvenot, *Angew. Chem*., 1996, **35**, 1961-1964.
4. R. Thouvenot, M. Fournier, R. Franck, C. Rocchioccioli-Deltcheff, *Inorg. Chem*., 1984, **23**, 598-605.
5. M. A. Fedotov, B. Z. Pertsikov, D. K. Danovich, *Polyhedron*, 1990, **9**, 1249-1256.
6. A. Zhang, R. C. Howell, K. B. Scotland, F. G. Perez, L. Todaro, L. C. Francesconi, *Inorg. Chem*., 2004, **43**, 7691-770.
7. J. Iijima, H. Naruke, *Inorg. Chim. Acta*, 2011, **379**, 95-99.
8. S. Himeno, M. Takamoto, *J. Electroanal. Chem.,* 2002, **528**, 170-174.
9. S. Himeno, M. Takamoto, A. Higuchi, M. Maekawa, *Inorg. Chim. Acta*, 2003, **348**, 57-62.
10. D. Barreca, G. Carta, A. Gasparotto, G. Rossetto, E. Tondello, P. Zanella, *Surf. Sci. Spectra*, 2001, **8**, 258-268.